MRS Advances © 2018 Materials Research Society DOI: 10.1557/adv.2018.604



Ultra-robust Superhydrophobic/superoleophilic Stainless Mesh Coated by PTFE/SiO₂ for Oil/water Separation

Chaolang Chen, Ding Weng, Awais Mahmood, Jiadao Wang

State Key Laboratory of Tribology, Tsinghua University, Beijing 100084, China

Abstract

In this study, a superhydrophobic and superoleophilic stainless mesh coated with $polytetra fluoro ethylene/silicon\ dioxide\ (PTFE/SiO_2)\ was\ fabricated\ through\ electrostatic\ self-polytetra fluoro ethylene/silicon\ dioxide\ (PTFE/SiO_2)\ was\ fabricated\ through\ electrostatic\ self-polytetra fluoro ethylene/silicon\ dioxide\ (PTFE/SiO_2)\ was\ fabricated\ through\ electrostatic\ self-polytetra fluoro ethylene/silicon\ dioxide\ (PTFE/SiO_2)\ was\ fabricated\ through\ electrostatic\ self-polytetra fluoro ethylene/silicon\ dioxide\ (PTFE/SiO_2)\ was\ fabricated\ through\ electrostatic\ self-polytetra fluoro ethylene/silicon\ dioxide\ (PTFE/SiO_2)\ was\ fabricated\ through\ electrostatic\ self-polytetra fluoro ethylene/silicon\ dioxide\ (PTFE/SiO_2)\ was\ fabricated\ through\ electrostatic\ self-polytetra fluoro ethylene/silicon\ dioxide\ (PTFE/SiO_2)\ was\ fabricated\ through\ electrostatic\ self-polytetra fluoro ethylene/silicon\ dioxide\ (PTFE/SiO_2)\ was\ fabricated\ through\ electrostatic\ self-polytetra fluoro\ ethylene/silicon\ dioxide\ (PTFE/SiO_2)\ was\ fabricated\ through\ electrostatic\ self-polytetra fluoro\ ethylene/silicon\ dioxide\ (PTFE/SiO_2)\ was\ fabricated\ through\ electrostatic\ self-polytetra fluoro\ ethylene/silicon\ ethylene/silicon$ assembly method followed by sintering treatment. The PTFE was utilized to construct lowsurface-energy surface and the SiO₂ nanoparticles were added to enhance its surface roughness. The as-prepared stainless mesh exhibited desirable superhydrophobicity and superoleophilicity with a water contact angle of 152° and oil contact angle of 0°. The coated stainless mesh could separate a variety of oil/water mixtures with high efficiency and it also exhibited good recyclability. Moreover, the corrosion-resistance of stainless mesh was greatly improved by coating it with PTFE. The thermogravimetric analysis (TGA) measurements showed that the coated mesh could withstand high temperature of up to 430°C, indicating excellent thermal-resistance. It is believed that this ultra-robust stainless mesh would have significant potential applications in industry.

INTRODUCTION

In the past decades, the separation of oil/water contamination has become one of most important and urgent global environmental problem [1-4]. The traditional methods including skimmers, air flotation and centrifugation are usually employed to separate oil and water. Nevertheless, those techniques are low-efficient, expensive and complicated, which greatly limit their development and usage in industry [5-7].

Currently, superhydrophobic/superoleophilic materials have increasing attention because of their advantages of high separation capacity, high selectivity, simplicity and cost-efficiency [8-10]. For example, fluorinated alkyl silane/TiO₂ modified fabric [11], PDMS-SiO₂ coated PET membrane [12], SiO₂-TMS modified PVDF membrane [13] and so on, have been developed and successfully applied for oil/water separation. However, most of the aforementioned superhydrophobic and superoleophilic surfaces would deteriorate their superhydrophobic performance when used in harsh environment such as strong corrosive and high temperature, thus limiting their applications in real oil/water separation. Therefore, it is of significance to develop superhydrophobic materials with excellent robustness which can be produced by a simple and cost-efficient method.

PTFE is considered to be a desirable candidate to construct robust superhydrophobic surface due to its intrinsic hydrophobicity, chemical and thermal stability [14-16]. In our previous papers [17,18], we reported superhydrophobic PTFE coated filter paper and PTFE nanofibers coated metal porous materials, which could separate types of oil/water mixtures. In this study, a superhydrophobic/superoleophilic stainless mesh coated with PTFE/SiO $_2$ is fabricated by simple self-assembly method. The as-prepared mesh can separate a variety of oil/water mixtures with high efficiency. Moreover, the anti-corrosive and high temperature resistance properties of obtained mesh are further investigated. It is believed that this PTFE/SiO $_2$ coated stainless mesh has important potential applications for oil/water separation.

EXPERIMENTAL SECTION

Materials

All materials were purchased commercially and were used without further purification. The PTFE nanoparticles (NPs) colloid solution with 60 wt% mass fraction and average 200 nm of particle size was purchased from 3F New Material Co. Ltd., China. The SiO₂ monodisperse suspension (average particle size 560nm, 2.5 wt%) was purchased from Tianjin BaseLine ChromTech Research Centre, China. The poly dimethyl diallyl ammonium chloride (PDDA), Sodium chloride and ethanol and acetone were obtained from Aladdin Industrial Co., Ltd., China. The gasoline was purchased from China National Petroleum Corporation, China. Decane, tetrachloromethane, silicone oil, trichloromethane, NaOH and H₂SO₄ (98 wt%, extra grade) were obtained from J&K, China. The water used in this work was ultra-pure water. The stainless mesh (400 mesh) was obtained from shanghai tongshi Co., Ltd., China. The meshes were cleaned by using ultrasonic cleaner, in acetone, ethanol and ultra-pure water for 15 min, respectively, and then dried by using nitrogen gas before use.

Fabrication of superhydrophobic stainless mesh

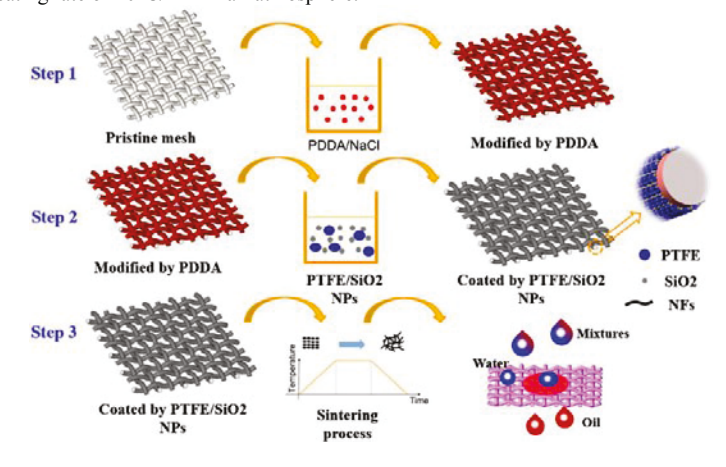
As shown in Figure 1, the fabrication process of superhydrophobic stainless mesh involves three steps. Firstly, the cleaned mesh was positively charged modified by immersing in PDDA (0.4 wt%)/NaCl (0.05 mM) solution for 10 min. Secondly, PTFE (6wt%) and SiO $_2$ (560nm lwt%) composite aqueous solution was sufficiently stirred to make a homogeneous suspension. After that, the PDDA modified mesh was steeped in the composite suspension for 15min. During this process, the PTFE/SiO $_2$ NPs spontaneously moved to the metal wires surface driven by electrostatic force and formed PTFE/SiO $_2$ NPs coating. Finally, the PTFE/SiO $_2$ NPs coated mesh was sintered at 380°C in furnace (GSL1500X) for 1h and cooled down in air to form PTFE nanofibers/SiO $_2$ coating on stainless mesh.

Oil/water separation

The as-prepared mesh was fixed between glass tubes. A mixture of 10 mL oil (dyed with methyl red) and 10 mL of water was slowly poured into the upper glass tube. The separation efficiency was calculated by using the ratio of the mass of water before and after separation process according to the equation: $\eta\text{=}m/m_{_0}\times100\%$, Where η is the separation efficiency, $m_{_0}$ is the mass of the water before separation and m is the mass of the water after separation.

Characterization

The morphology of pristine and coated mesh were observed by HITACHI SU8220 field emission scanning electron microscope. The chemical composition was analysed by the energy dispersive spectroscopy (EDS). All measurements of water contact angle (WCA) and water sliding angle (WSA) were conducted using an OCA 25 machine (Data-Physics, Germany) at room temperature. The volume of water used for measurements of WCA and WSA was 3 μL and 10 μL , respectively. The average value of at least three measurements performed at different positions on the same sample was adopted as the WCA or WSA. The measurement of Tafel plots was performed on electrochemical workstation (EG&G273A). The TGA data were obtained using a thermogravimetric analysis (STA73000, Beijing SaiSiMeng Instruments Co., Ltd) at a heating rate of 10°C/min in air atmosphere.



 $\textbf{Figure 1}. \ \textbf{The schematic diagrams of fabrication of PTFE/SiO}_2 \ coated \ stainless \ mesh.$

RESULTS AND DISCUSSIONS

Morphologies of pristine and PTFE/SiO2 coated stainless mesh

Scanning electron microscopy (SEM) was performed to evaluate the morphologies of pristine and PTFE/SiO $_2$ coated stainless mesh. As shown in Figure 2(a, b), the surface of pristine mesh was smooth with an average diameter of 40 μ m. After coated with PTFE/SiO $_2$ and sintering treatment, the metal wires of mesh were completely

wrapped by a dense and uniform PTFE nanofibers layer, and SiO₂ nanoparticles distributed randomly on the surface (Figure 2(c-e)). The transformation of PTFE nanofibers from PTFE nanoparticles was resulted from a liquid-crystal "templating" mechanism [19-21]. Moreover, from figure 2f, it is can be seen that the SiO₂ nanoparticles were embed into the PTFE nanofibrous coating and they provided a rough structure on a nano-scale level. The surface chemical composition of pristine and coated stainless mesh was also examined by energy-dispersive spectroscopy (EDS). The spectrum of pristine mesh exhibits peaks for carbon, ferrum, silicon and chromium, but no oxygen and fluorine elements were detected (Figure 3a). Moreover, an EDS scan of coated mesh yields carbon, ferrum, silicon, chromium, oxygen and elements (Figure 3b). The appearance of peaks of fluorine and the increase of carbon in coated mesh can be attributed to the presence of PTFE. Similarly, the appearance of peaks of oxygen and the increase of silicon demonstrated the existence of SiO2. Besides, the EDS mapping tests of carbon, fluorine, oxygen and silicon were carried out to evaluate their distribution on coated mesh (Figure 3c). The distributions of carbon and fluorine reveal that the mesh wires were thoroughly wrapped by a homogeneous layer of PTFE with thickness of around 0.3~1.5 μm. The distribution of oxygen and silicon indicated that the SiO₂ nanoparticles distribute randomly on the surface.

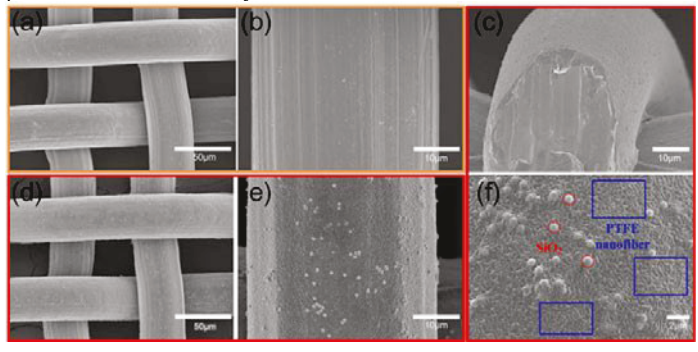


Figure 2. SEM images of pristine mesh (a, b) and the coated mesh (d, e, f); (c) the cross profile of coated mesh.

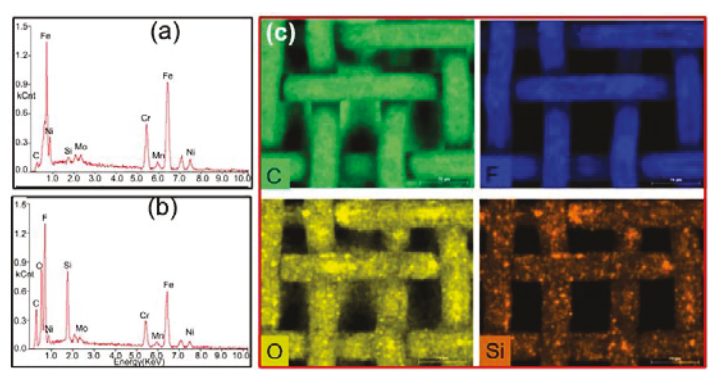


Figure 3. (a) The EDS test of pristine stainless mesh; (b) the EDS test of coated stainless mesh; (c) the EDS mapping tests of coated stainless mesh.

Wettability

The surface wettability was estimated by the measurement of water and oil contact angles. The pristine mesh showed slightly hydrophobic characteristic with an average WCA of 100° (Figure 4(a, b)). However, after coated with PTFE/SiO₂, it can be seen that all water droplets sitting on the coated mesh are ball-shaped and exhibit a WCA of 152° (Figure 4(c, d)). A jet of water could bounce off the as-prepared mesh without leaving residual, indicating the weak interaction between water and coated mesh surface (Figure 4e). The water droplets could easily roll off from the slightly tilted coated mesh surface (Figure 4f). All these results demonstrated that the as-prepared stainless mesh become superhydrophobic because of the presence of low-surface-energy PTFE and hierarchical roughness structure. On the contrary, when an oil droplet (decane) was dropped onto the as-prepared mesh in air, the oil droplet could quickly spread on the surface, exhibiting superoleophilic property (Figure 5a). Besides, when the coated mesh was immersed in the water, it also showed superoleophilicity. Therefore, it can be concluded that the as-prepared stainless mesh possesses superoleophilic property in both air and water medium.

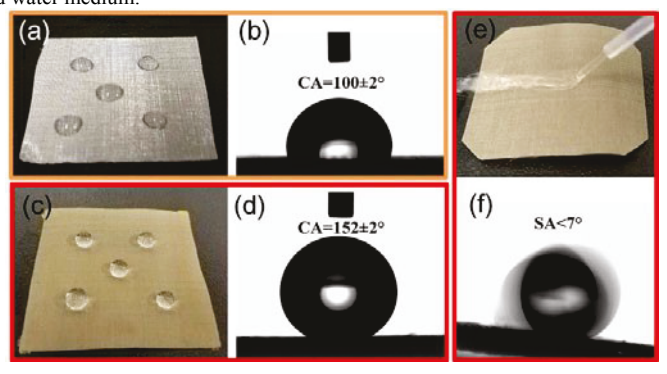


Figure 4. Images of water droplet on pristine and coated stainless mesh: (a) Optical image of water droplets on pristine mesh; (b) the WCA measurement of pristine mesh; (c) optical image of water droplets on coated mesh; (d) WCA test of coated mesh; (e) a jet of water bouncing off the coated mesh; (f) the rolling state of water droplet on a tilted coated mesh.

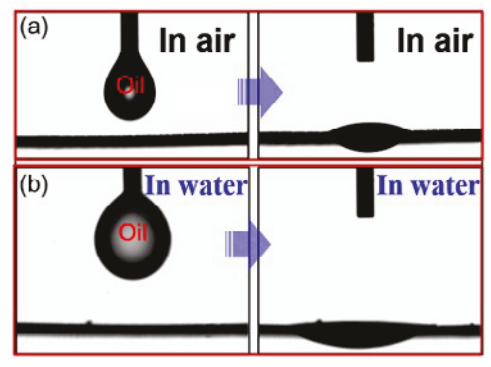


Figure 5. The measurements of oil contact angles of as-prepared mesh in air (a) and water (b) phase.

Oil/water separation

By utilizing the superhydrophobic and superoleophilic properties of the coated mesh, it can be used as a superb candidate for oil/water separation. To demonstrate the feasibility of as-prepared mesh for separating oil and water, a series of tests were carried out. As shown in Figure 6, the as-prepared mesh was fixed between two glass tubes and the oil/water mixtures was carefully poured into the upper tube. The oil (dyed with methyl red) quickly passed through the coated mesh and dropped into the collection beaker underneath, while the water was repelled and remained in the upper glass tube. Other types of mixtures including decane/water, tetrachloromethane/water, silicon oil/water, gasoline/water and trichloromethane/water were also successfully separated with high efficiency of above 98% (Figure 7a). In addition, the as-prepared mesh has great performance on recyclability. After each oil/water separation experiment, the asprepared mesh was rinsed with alcohol and water to remove the adsorbed oil. The asprepared mesh maintained more than 98% separation efficiency after 30 separation cycles for the tetrachloromethane/water mixture (Figure 7b). in addition to this, the surface of as-prepared mesh maintained its highly hydrophobicity with a WCA of 146.6° after 30 cycles of oil/water filtration, showing excellent recyclability for oil/water separation without significant changes of superhydrophobicity and separation efficiency.



Figure 6. The separation process for oil/water mixtures

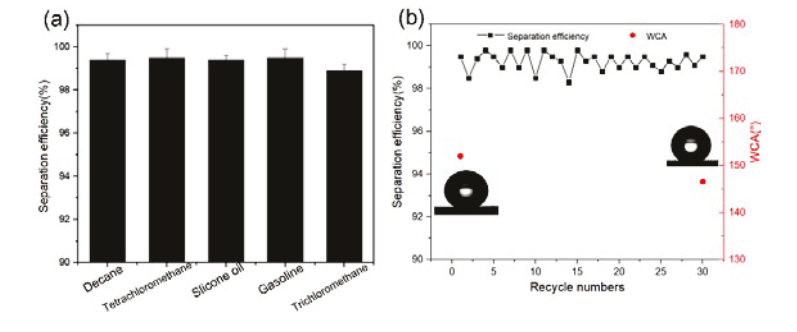


Figure 7. (a) The separation efficiency of as-prepared mesh for types of oil/water mixtures; (b) the effect of cycle time on the separation efficiency and WCA of as-prepared mesh.

Evaluation of corrosive resistance and thermal-resistance

The anti-corrosive property of as-prepared mesh was investigated by carrying out polarization measurements. The corrosion characteristics of pristine and coated mesh in 0.5 M H₂SO₄ solution, 3.5 wt% NaCl aqueous solution and 1 M NaOH solution were given in Table 1 and the Tafel plots were shown in Figure 8(a-c). According to table 1, the i_{corr} values of pristine mesh appeared to be relatively high in both H_2SO_4 and NaCl aqueous solution. This was attributed to the pristine mesh surfaces that it is at unstable state and iron ionize quickly, resulting in the surfaces suffering from corrosion. Meanwhile, the corrosive potential of coated mesh was found to be relatively higher than that of pristine mesh. The shift of the corrosive potential in the positive direction demonstrated that the PTFE/SiO2 coating act as anodic protective coating rather than the sacrificial corrosion protective. Furthermore, the coated mesh was immersed in 0.5 M H₂SO₄ for 100 h to examine its anti-corrosive. The results indicated that the surface of coated mesh had no obvious change and still exhibit superhydrophobicity (Figure 8d). When the coated mesh was tested in 1 M NaOH solution, the corrosion current in coated mesh was much higher than that of pristine mesh (Table 1). This is because that the SiO₂ nanoparticles were dissolved by NaOH, leading to high corrosive current. The SEM image of coated mesh after immersed in 1 M NaOH solution for 100 h showed that the superficial SiO2 nanoparticles were thoroughly removed by NaOH and it left nanoholes on the coating surface (Figure 8e). Nevertheless, the PTFE coating still showed no obvious change and the mesh maintained high hydrophobicity with WCA of 148°. It is believed that the PTFE coating serve as an effective barrier to the inward diffusion of corrosive ion, thus protecting the substrate from corrosion. All the results demonstrated that the PTFE/SiO₂ coated stainless mesh possesses excellent corrosion-resistant

Table 1. The corrosion characteristics on the surfaces of pristine and coated stainless mesh.

	0.5 M H ₂ SO ₄		3.5 wt% NaCl		1 M NaOH	
Samples	$E_{corr}(mV)$	$i_{corr}(A)$	$E_{corr}(mV)$	$i_{corr}(A)$	$E_{corr}(\text{mV})$	$i_{corr}(A)$
Pristine mesh	-31.486	7.08×10^{-5}	-117.5	7.08×10^{-7}	-246.19	4.92×10^{-7}
Coated mesh	79.67	1.9×10^{-5}	-86.547	5.93×10^{-7}	-95.7	2.48×10^{-2}

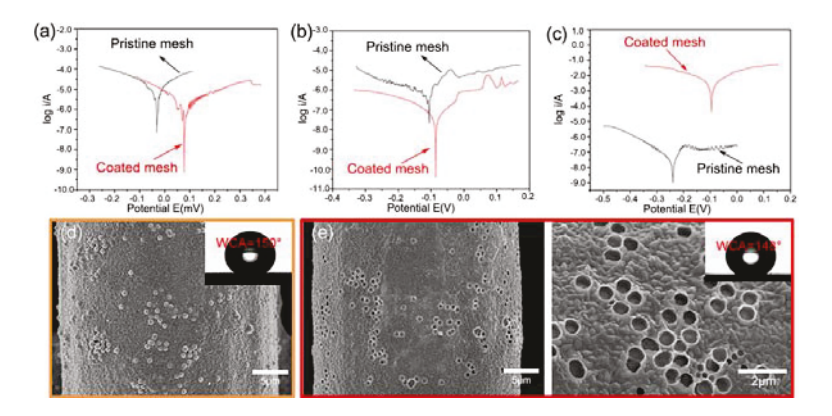


Figure 8. Tafel plots of pristine and coated stainless mesh in 0.5 M H₂SO₄ (a), 3.5wt% NaCl (b) and 1 M NaOH (c) aqueous solution; the SEM images of coated stainless mesh after immersed in 0.5 M H₂SO₄ (d), 1 M NaOH (e) aqueous solution for 100 h and the insets are the WCA.

Furthermore, the thermal stability of the coated stainless mesh was studied by thermogravimetric analysis. As shown in Figure 9a, when the temperature was less than 430°C, the as-prepared mesh showed a stable behaviour and the weight had no obvious changes, indicating excellent thermal-resistant property. In addition, the as-prepared mesh was placed in a furnace and heated at 400°C for few hours before the measurements of WCA, the results showed that the oil/water separation efficiency and WCA remain almost unchanged (Figure 9b). Therefore, it is believed that the superhydrophobic stainless mesh with outstanding anti-corrosion and thermal-resistance would be an excellent engineering material for industrial applications.

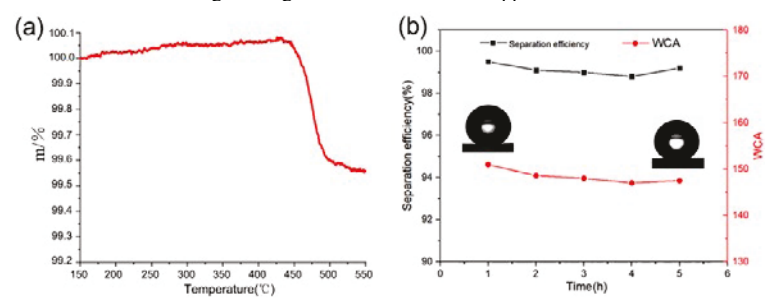


Figure 9. (a) The TGA curve of as-prepared stainless mesh; (b) the variation of separation efficiency and WCA of asprepared stainless mesh exposed at 400°C.

CONCLUSIONS

In summary, we developed a superhydrophobic and superoleophilic stainless mesh that was fabricated by utilizing electrostatic self-assembly followed by sintering

and recyclability. Moreover, the corrosion-resistance property of pristine and coated mesh was investigated by polarization measurements and the results indicated that the coated stainless mesh showed excellent anti-corrosion properties in various corrosive mediums including strong acidic, salt and alkaline solutions. The coated mesh exhibited outstanding thermal-resistance and could withstand high temperature up to 430°C. Thereby, this as-prepared stainless mesh with ultra-robust properties to corrosive solution and extreme high temperature would have important industrial applications.

process. The as-prepared stainless mesh exhibited high oil/water separation efficiency

ACKNOWLEDGMENTS

We thank the funding support from National Natural Science Foundation of China Project under grant nos. 51375253 and 51775296. We also acknowledge the support of this work from the Tsinghua National Laboratory for Information Science and Technology, China.

REFERENCES

- S. J. Gao, Z. Shi, W. B. Zhang, F. Zhang, and J. Jin, Acs Nano, 8, 6344-6352 (2014).
 X. Gao, L. P. Xu, Z. Xue, L. Feng, J. Peng, Y. Wen, S. Wang, X. Zhang, Adv. Mater, 26, 1771-1775 (2014).
 S. Chen, J. Wang, and D. Chen, Mrs Adv, 1, 667-673 (2016).
 J. L. Ge, D. D. Zong, Q. Jin, J. Y. Yu, and B. Ding, Adv. Funct. Mater, 28, 1705051(2018).
 W. Qing, X. Shi, Y. Deng, W. Zhang, J. Wang, and C. Y. Tang, J. Membr. Sci, 540, 354-361

- J. L. Ge, D. D. Zong, Q. Jin, J. Y. Yu, and B. Ding, Adv. Funct. Mater, 28, 1705051(2018).
 W. Qing, X. Shi, Y. Deng, W. Zhang, J. Wang, and C. Y. Tang, J. Membr. Sci, 540, 354-361 (2017).
 K. Yin, D. Chu, X. Dong, C. Wang, J. Duan, and J. He, Nanoscale. 9, 14229-14235 (2017).
 J. J. Zhang, F. Wang, Z. Li, J. Yu, and B. Ding, J. Mater. Chem. A, 5, 497-502 (2016).
 J. Song, S. Huang, Y. Lu, X. Bu, J. E. Mates, A. Ghosh, R. Ganguly, C. J. Carmalt, I. P. Parkin, W. Xu, and C. M. Megaridis, ACS Appl. Mater. Interfaces, 6, 19858-19865 (2014).
 X. Zhou, Z. Zhang, X. Xu, G. Fang, X. Zhu, X. Men and B. Ge, ACS Appl. Mater. Interfaces, 5, 7208-7214 (2013).
 M. Tao, L. Xue, F. Liu, and L. Jiang, Adv. Mater, 26, 2943-2948 (2014).
 J. Y. Huang, S. H. Li, M. Z. Ge, L. N. Wang, T. L. Xing, G. Q. Chen, X. F. Liu, S. S. Al-Deyab, Q. Zhang, T. Chen and Y. K. Lai, J. Mater. Chem. A, 3, 2825-2832 (2015).
 W. H. Sang, K. D. Kim, H. O. Seo, I. H. Kim, S. J. Chan, J. E. An, J. H. Kim, S. Uhm, and Y. D. Kim, Macromol. Mater. Eng, 302, 1700218 (2017).
 J. Ju, T. Wang, and Q. Wang, J. Appl Polym. Sci, 132, 42077 (2015).
 J. Yong, Y. Fang, F. Chen, J. Huo, Q. Yang, H. Bian, G. Du and X. Hou, Appl Surf Sci, 389, 1148-1155 (2016).
 J. Cheng, W. Hou, Q. Wang, and T. Wang, Appl Surf Sci, 257, 4821-4825 (2011).
 L. Feng, Z. Zhang, Z. Mai, Y. Ma, B. Liu, L. Jiang and D. Zhu, Angew. Chem. Int. Ed, 43, 2012-2014 (2004).
 C. Chen, C. Du, D. Weng, A. Mahmood, D. Feng, and J. Wang, ACS Appl. Nano. Mater, 1, 2632-2639 (2018).
 Z. Luo, Z. Zhang, W. Wang, W. Liu, and Q. Xue, Mater. Chem. Phys, 119, 40-47 (2010).
 C. T. Kresge, M. E. Leonowicz, W. J. Roth, J. C. Vartuli, and J. S. Beck, Nature, 359, 710-712 (1992).
 Z. Luo, Z. Zhang, L. T. Hu, W. M. Liu, Z. G. Guo, H. J. Zhang and W. J. Wang, Adv.

- (1992). **21.** Z. Z. Luo, Z. Z. Zhang, L. T. Hu, W. M. Liu, Z. G. Guo, H. J. Zhang and W. J. Wang, Adv. Mater, 20, 970-974 (2008).